

Nodeless superconducting gaps in $\text{Ca}_{10}(\text{Pt}_{4-\delta}\text{As}_8)((\text{Fe}_{1-x}\text{Pt}_x)_2\text{As}_2)_5$ probed by quasiparticle heat transport

X. Qiu, L. P. He, X. C. Hong, Z. Zhang, J. Pan, X. P. Shen, D. L. Feng, and S. Y. Li*
*State Key Laboratory of Surface Physics, Department of Physics,
 and Laboratory of Advanced Materials,
 Fudan University, Shanghai 200433, P. R. China*

(Dated: May 10, 2019)

The in-plane thermal conductivity of iron-based superconductor $\text{Ca}_{10}(\text{Pt}_{4-\delta}\text{As}_8)((\text{Fe}_{1-x}\text{Pt}_x)_2\text{As}_2)_5$ single crystal (“10-4-8”, $T_c = 22$ K) was measured down to 80 mK. In zero field, the residual linear term κ_0/T is negligible, suggesting nodeless superconducting gaps in this multiband compound. In magnetic fields, κ_0/T increases rapidly, which mimics those of multiband superconductor NbSe_2 and $\text{LuNi}_2\text{B}_2\text{C}$ with highly anisotropic gap. Such a field dependence of κ_0/T is an evidence for multiple superconducting gaps with quite different magnitudes or highly anisotropic gap. Comparing with the London penetration depth results of $\text{Ca}_{10}(\text{Pt}_3\text{As}_8)((\text{Fe}_{1-x}\text{Pt}_x)_2\text{As}_2)_5$ (“10-3-8”) compound, the 10-4-8 and 10-3-8 compounds may have similar superconducting gap structure.

PACS numbers: 74.70.Xa, 74.25.fc

I. INTRODUCTION

To understand the electronic pairing mechanism of a superconductor, it is very important to know the symmetry and structure of its superconducting gap. For the iron-based high-temperature superconductors, there are many families, such as $\text{LaO}_{1-x}\text{F}_x\text{FeAs}$ (“1111”),¹ $\text{Ba}_{1-x}\text{K}_x\text{Fe}_2\text{As}_2$ (“122”),² $\text{NaFe}_{1-x}\text{Co}_x\text{As}$ (“111”),³ and $\text{FeSe}_x\text{Te}_{1-x}$ (“11”).⁴ The most notable character of these families is the multiple Fermi surfaces, which may be the reason why their superconducting gap structure is so complicated.^{5,6}

Different from other families, the new compounds $\text{Ca}_{10}(\text{Pt}_3\text{As}_8)((\text{Fe}_{1-x}\text{Pt}_x)_2\text{As}_2)_5$ (“10-3-8”) and $\text{Ca}_{10}(\text{Pt}_4\text{As}_8)((\text{Fe}_{1-x}\text{Pt}_x)_2\text{As}_2)_5$ (“10-4-8”) consist of semiconducting $[\text{Pt}_3\text{As}_8]$ layers or metallic $[\text{Pt}_4\text{As}_8]$ layers sandwiched between $[\text{Fe}_{10}\text{As}_{10}]$ layers, and show superconductivity with maximal $T_c \sim 15$ and 38 K, respectively.⁷⁻⁹ The metallic $[\text{Pt}_4\text{As}_8]$ layers lead to stronger FeAs interlayer coupling in 10-4-8 compound, thus higher T_c as compared to the 10-3-8 compound.⁸ The upper critical field of both 10-3-8 and 10-4-8 compounds show strong anisotropy.^{10,11} For the 10-3-8 compound, the London penetration depth exhibits power-law variation, which suggests nodeless superconducting gap.¹² For the 10-4-8 compound, the angle-resolved photoemission spectroscopy (ARPES) experiments have revealed a multiband electronic structure,^{13,14} but so far there is still no any investigation of its superconducting gap structure. As the 10-4-8 has a much higher T_c than the 10-3-8 compound, it will be interesting to study its superconducting gap structure and compare with the 10-3-8 compound.

Low-temperature thermal conductivity measurement is a bulk technique to study the superconducting gap structure.¹⁵ According to the magnitude of residual linear term κ_0/T in zero field, one may judge whether there

exist gap nodes or not. The field dependence of κ_0/T can give further information on nodal gap, gap anisotropy, or multiple gaps.¹⁵

In this paper, we measure the thermal conductivity of $\text{Ca}_{10}(\text{Pt}_{4-\delta}\text{As}_8)((\text{Fe}_{1-x}\text{Pt}_x)_2\text{As}_2)_5$ ($T_c = 22$ K) single crystal down to 80 mK. A negligible residual linear term κ_0/T is found in zero magnetic field. The field dependence of κ_0/T is very similar to those in multigap s -wave superconductor NbSe_2 and $\text{LuNi}_2\text{B}_2\text{C}$ with highly anisotropic gap. Our data strongly suggest $\text{Ca}_{10}(\text{Pt}_{4-\delta}\text{As}_8)((\text{Fe}_{1-x}\text{Pt}_x)_2\text{As}_2)_5$ has nodeless superconducting gaps. The magnitudes of these gaps could be quite different, or some gap may be anisotropic.

II. EXPERIMENT

Single crystals of $\text{Ca}_{10}(\text{Pt}_{4-\delta}\text{As}_8)((\text{Fe}_{1-x}\text{Pt}_x)_2\text{As}_2)_5$ ($T_c = 22$ K) were grown by the flux method.¹³ The composition of the sample was determined as Ca:Fe:Pt:As = 2:1.73:0.79:3.39 by wavelength-dispersive spectroscopy (WDS), utilizing an electron probe micro-analyzer (Shimadzu EPMA-1720). This doping level is close to the $T_c = 26$ K sample with Ca:Fe:Pt:As = 2:1.8:0.9:3.5 in Ref. 8, which has the chemical formula $\text{Ca}_{10}(\text{Pt}_{4-\delta}\text{As}_8)((\text{Fe}_{0.97}\text{Pt}_{0.03})_2\text{As}_2)_5$ ($\delta = 0.26$) determined by single crystal structure refinement. The dc magnetization was measured at $H = 20$ Oe, with zero-field cooling process, using a SQUID (MPMS, Quantum Design).

The sample was cleaved to a rectangular shape with dimensions of 1.5×0.74 mm² in the ab plane and ~ 25 μm along the c axis. Contacts were made directly on the fresh sample surfaces with silver paint, which were used for both resistivity and thermal conductivity measurements. In-plane thermal conductivity was measured in a dilution refrigerator using a standard four-wire steady-

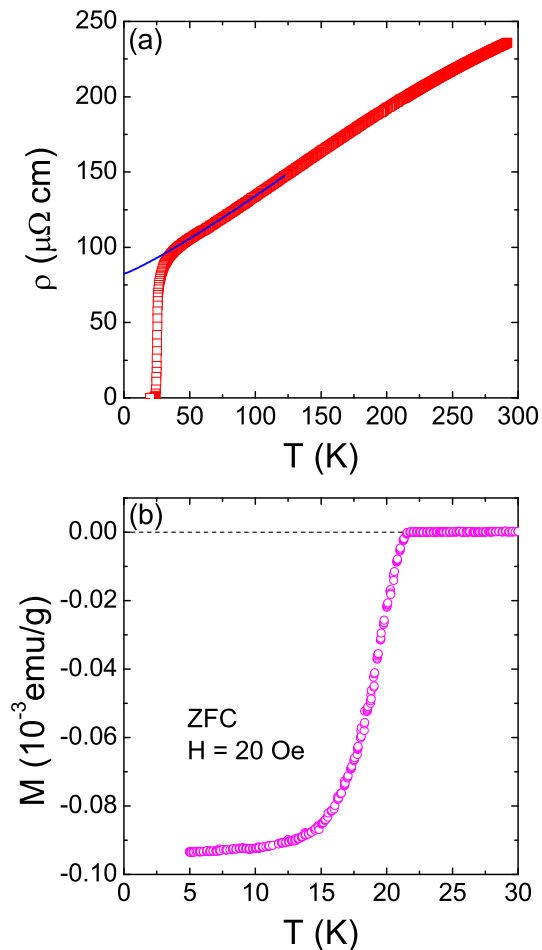


FIG. 1. (Color online) (a) In-plane resistivity $\rho(T)$ of $\text{Ca}_{10}(\text{Pt}_{4-\delta}\text{As}_8)((\text{Fe}_{1-x}\text{Pt}_x)_2\text{As}_2)_5$ single crystal in zero field. The solid line is a fit of the data between 50 and 125 K to $\rho = \rho_0 + AT^\alpha$. (b) Low-temperature magnetization of $\text{Ca}_{10}(\text{Pt}_{4-\delta}\text{As}_8)((\text{Fe}_{1-x}\text{Pt}_x)_2\text{As}_2)_5$ single crystal measured in $H = 20$ Oe, with the zero-field-cooled (ZFC) process.

state method with two RuO_2 chip thermometers, calibrated *in situ* against a reference RuO_2 thermometer. Magnetic fields are applied along the c axis. To ensure a homogeneous field distribution in the samples, all fields are applied at a temperature above T_c .

III. RESULTS AND DISCUSSION

Figure 1(a) shows the in-plane resistivity of $\text{Ca}_{10}(\text{Pt}_{4-\delta}\text{As}_8)((\text{Fe}_{1-x}\text{Pt}_x)_2\text{As}_2)_5$ single crystal in zero field. Defined by $\rho = 0$, $T_c = 22.2$ K is obtained. The solid line is a fit of the data between 50 and 125 K to $\rho = \rho_0 + AT^\alpha$, which gives residual resistivity $\rho_0 = 82.5 \mu\Omega \text{ cm}$ and $\alpha = 1.15$. The dc magnetization is shown in Fig. 1(b), and a slightly lower $T_c = 21.7$ K is found. Below we take $T_c = 22$ K. This value is lower than the $T_c = 38$ K at optimal doping. Since the phase diagram, T_c vs $x(\delta)$, of 10-4-8 system has not been well

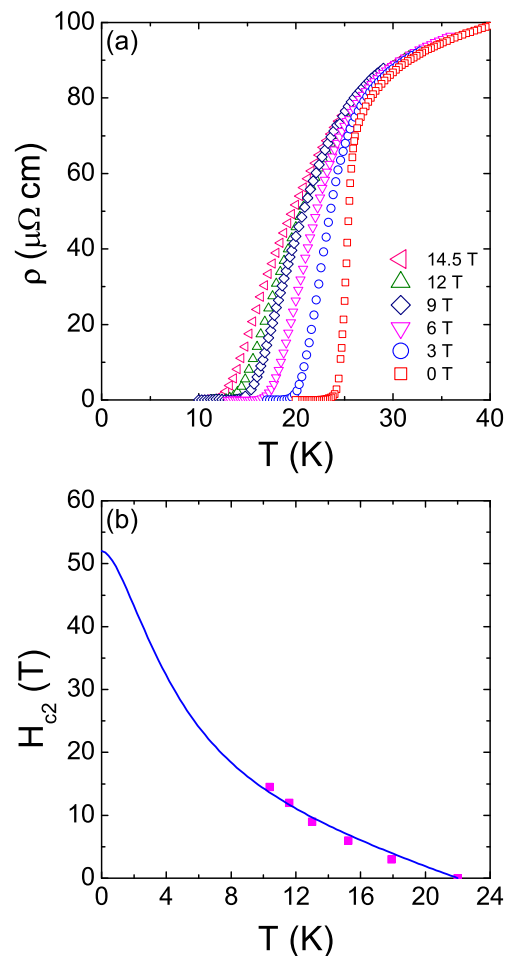


FIG. 2. (Color online) (a) Low-temperature resistivity of $\text{Ca}_{10}(\text{Pt}_{4-\delta}\text{As}_8)((\text{Fe}_{1-x}\text{Pt}_x)_2\text{As}_2)_5$ single crystal in magnetic fields ($H = 0, 3, 6, 9, 12,$ and 14.5 T) along the c axis. (b) Temperature dependence of the upper critical field $H_{c2}(T)$. The solid line is a fit to the two-band model,^{11,17} which points to $H_{c2}(0) \approx 52$ T.

studied, it is not sure that our sample is underdoped or overdoped.

Figure 2(a) shows the low-temperature resistivity of $\text{Ca}_{10}(\text{Pt}_{4-\delta}\text{As}_8)((\text{Fe}_{1-x}\text{Pt}_x)_2\text{As}_2)_5$ single crystal in magnetic fields up to 14.5 T. The superconducting transition becomes broader and the T_c decreases with increasing field. The temperature dependence of upper critical field $H_{c2}(T)$, defined by $\rho = 0$ in Fig. 2(a), is plotted in Fig. 2(b). To estimate the zero-temperature limit of H_{c2} , one usually fits the curve according to the Werthamer-Helfand-Hohenberg (WHH) theory.¹⁶ However, our $H_{c2}(T)$ with upward curvature apparently can not be fitted well by WHH formula. As explained in Ref. 11, the underlying reason is that the WHH theory is for superconductors with single band, while the iron-based superconductors have multiple bands. In Ref. 11, the $H_{c2}^{\parallel c}(T)$ curve of $\text{Ca}_{10}(\text{Pt}_{4-\delta}\text{As}_8)((\text{Fe}_{0.97}\text{Pt}_{0.03})_2\text{As}_2)_5$ ($T_c = 26$ K) sample was fitted by the two-band model,¹⁷

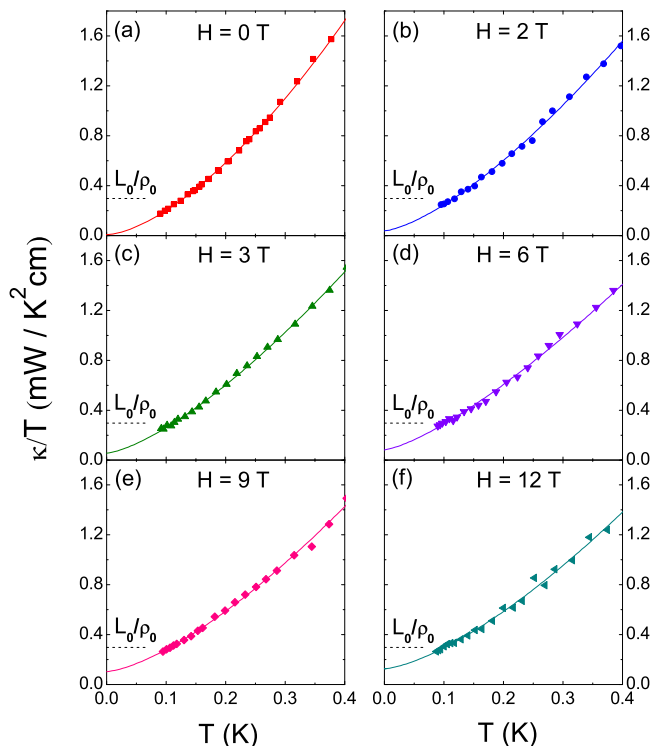


FIG. 3. (Color online) Low-temperature thermal conductivity of $\text{Ca}_{10}(\text{Pt}_{4-\delta}\text{As}_8)((\text{Fe}_{1-x}\text{Pt}_x)_2\text{As}_2)_5$ with magnetic fields applied along the c axis ($H = 0, 2, 3, 6, 9,$ and 12 T). The solid lines are $\kappa/T = a + bT^{\alpha-1}$ fits, and the dashed line is the normal-state Wiedemann-Franz law expectation L_0/ρ_0 .

giving $H_{c2}^{\parallel c}(0) \approx 90$ T. Taking the same process as in Ref. 11, we also fit the $H_{c2}(T)$ data in Fig. 2(b) with the two-band model, and get $H_{c2}(0) = 52$ T for our $\text{Ca}_{10}(\text{Pt}_{4-\delta}\text{As}_8)((\text{Fe}_{1-x}\text{Pt}_x)_2\text{As}_2)_5$ ($T_c = 22$ K) sample. Note that a slightly different $H_{c2}(0)$ does not affect our discussion on the field dependence of normalized κ_0/T blow.

In Fig. 3, the temperature dependence of the in-plane thermal conductivity for $\text{Ca}_{10}(\text{Pt}_{4-\delta}\text{As}_8)((\text{Fe}_{1-x}\text{Pt}_x)_2\text{As}_2)_5$ in $H = 0, 2, 3, 6, 9,$ and 12 T magnetic fields are plotted as κ/T vs T . To get the residual linear term κ_0/T , we fit the curves to $\kappa/T = a + bT^{\alpha-1}$ blow 0.4 K, in which the two terms aT and bT^{α} come from contributions of electrons and phonons, respectively.^{18,19} The power α of the phonon term is typically between 2 and 3, due to the specular reflections of phonons at the sample surfaces.^{18,19} In zero field, the fitting gives $\kappa_0/T = 0.005 \pm 0.013$ mW $\text{K}^{-2} \text{cm}^{-1}$ and $\alpha = 2.57 \pm 0.03$. Such a tiny value of κ_0/T is within our experimental error bar ± 0.005 mW $\text{K}^{-2} \text{cm}^{-1}$.¹⁹ Therefore it is negligible, comparing to the normal-state Wiedemann-Franz law expectation $L_0/\rho_0 = 0.297$ mW $\text{K}^{-2} \text{cm}^{-1}$, with $L_0 = 2.45 \times 10^{-8}$ $\text{W}\Omega \text{K}^{-2}$ and $\rho_0 = 82.5$ $\mu\Omega \text{cm}$. The absence of κ_0/T in zero field means that there are no fermionic quasiparticles to conduct heat as $T \rightarrow 0$, which provides

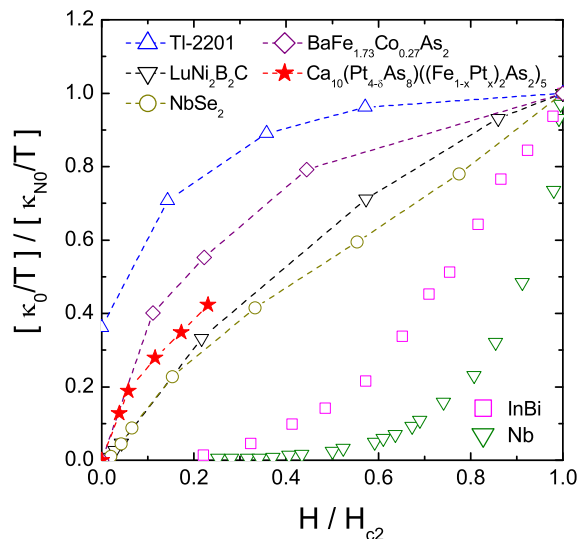


FIG. 4. (Color online) Normalized residual linear term κ_0/T of $\text{Ca}_{10}(\text{Pt}_{4-\delta}\text{As}_8)((\text{Fe}_{1-x}\text{Pt}_x)_2\text{As}_2)_5$ as a function of H/H_{c2} . For comparison, similar data are shown for the clean s -wave superconductor Nb,²⁰ the dirty s -wave superconducting alloy InBi,²¹ the multiband s -wave superconductor NbSe₂,²² the s -wave superconductor LuNi₂B₂C with highly anisotropic gap,²³ an overdoped d -wave cuprate superconductor Tl-2201,²⁴ and the iron-based superconductor BaFe_{1.73}Co_{0.27}As₂.²⁵

bulk evidence for nodeless superconducting gaps in $\text{Ca}_{10}(\text{Pt}_{4-\delta}\text{As}_8)((\text{Fe}_{1-x}\text{Pt}_x)_2\text{As}_2)_5$, at least in the ab plane. The data in magnetic fields $H = 2, 3, 6, 9,$ and 12 T are also fitted, as seen in Figs. 3(b)-3(f). The κ_0/T increases significantly with increasing field, although the maximum applied field $H = 12$ T is only about 23% of the $H_{c2}(0) = 52$ T.

To see the field dependence of κ_0/T more clearly, the normalized κ_0/T of $\text{Ca}_{10}(\text{Pt}_{4-\delta}\text{As}_8)((\text{Fe}_{1-x}\text{Pt}_x)_2\text{As}_2)_5$ as a function of H/H_{c2} is plotted in Fig. 4. Similar data are shown for the clean s -wave superconductor Nb,²⁰ the dirty s -wave superconducting alloy InBi,²¹ the multiband s -wave superconductor NbSe₂,²² the s -wave superconductor LuNi₂B₂C with highly anisotropic gap,²³ an overdoped d -wave cuprate superconductor Tl₂Ba₂CuO_{6+δ} (Tl-2201),²⁴ and the iron-based superconductor BaFe_{1.73}Co_{0.27}As₂.²⁵ For clean s -wave superconductor with a single isotropic gap, κ_0/T is expected to grow exponentially with increasing H , as found in Nb.²⁰ In a d -wave superconductor, κ_0/T increases roughly proportional to \sqrt{H} at low field due to the Volovik effect,²⁶ as found in Tl-2201.²⁴

From Fig. 4, the normalized κ_0/T of our 10-4-8 compound starts from a negligible value at zero field, then increases very rapidly with increasing field. This behavior clearly mimics those of NbSe₂ and LuNi₂B₂C.^{22,23} For the multiband s -wave superconductor NbSe₂, the gap on the Γ band is approximately one third of the gap on the other two Fermi surfaces and magnetic field

first suppresses the superconductivity on the Fermi surface with smaller gap.²² For the *s*-wave superconductor LuNi₂B₂C with highly anisotropic gap, the gap minimum Δ_{min} is at least 10 times smaller than the gap maximum, $\Delta_{min} \leq \Delta_0/10$.²³ The nearly identical field dependence of normalized κ_0/T between NbSe₂ and LuNi₂B₂C indicates that bulk thermal conductivity measurement can not distinguish these two kinds of superconducting gap structures. Nevertheless, the field dependence of κ_0/T suggests that the nodeless superconducting gaps in multiband 10-4-8 compound may have quite different magnitudes, or some gap could be anisotropic. Note that similar field dependence of κ_0/T was also observed in iron-based superconductors BaFe_{1.73}Co_{0.27}As₂ and FeSe_{*x*}.^{25,27}

In a theoretical calculation of $\kappa_0(H)/T$ with unequal size of isotropic s_{\pm} -wave gaps, the shape of $\kappa_0(H)/T$ changes systematically with the gap size ratio Δ_S/Δ_L .²⁸ In case of isotropic *s*-wave gaps with unequal size, the ratio $\Delta_S/\Delta_L \approx 1/4$ is estimated for our 10-4-8 compound, by comparing with the theoretical curves. However, we can not rule out that some gap may be anisotropic. In fact, the robust power-law variation of London penetration depth observed in 10-3-8 compound was interpreted as a multigap behavior, and the anisotropy of some superconducting gaps may increase towards the edges of the superconducting dome.¹² In the sense that both ther-

mal conductivity and London penetration depth measurements are bulk probe of the low-energy quasiparticles, the 10-4-8 and 10-3-8 compounds may have similar superconducting gap structure.

IV. SUMMARY

In summary, we have measured the thermal conductivity of Ca₁₀(Pt_{4- δ} As₈)((Fe_{1-*x*}Pt_{*x*})₂As₂)₅ single crystal down to 80 mK. The absence of κ_0/T in zero field gives strong evidence for nodeless superconducting gaps in such a multiband compound. The rapid field dependence of κ_0/T suggests multiple superconducting gaps with quite different magnitudes or highly anisotropic gap, which may be similar to that of Ca₁₀(Pt₃As₈)((Fe_{1-*x*}Pt_{*x*})₂As₂)₅ compound.

ACKNOWLEDGEMENTS

This work is supported by the Natural Science Foundation of China, the Ministry of Science and Technology of China (National Basic Research Program No. 2012CB821402), and the Program for Professor of Special Appointment (Eastern Scholar) at Shanghai Institutions of Higher Learning.

* E-mail: shiyan_li@fudan.edu.cn

-
- ¹ Y. Kamihara, T. Watanabe, M. Hirano, and H. Hosono, *J. Am. Chem. Soc.* **130**, 3296 (2008).
- ² M. Rotter, M. Tegel, and D. Johrendt, *Phys. Rev. Lett.* **101**, 107006 (2008).
- ³ D. R. Parker, M. J. P. Smith, T. Lancaster, A. J. Steele, I. Franke, P. J. Baker, F. L. Pratt, M. J. Pitcher, S. J. Blundell, and S. J. Clarke, *Phys. Rev. Lett.* **104**, 057007 (2010).
- ⁴ B. C. Sales, A. S. Sefat, M. A. McGuire, R. Y. Jin, D. Mandrus, and Y. Mozharivskiy, *Phys. Rev. B* **79**, 094521 (2009).
- ⁵ P. J. Hirschfeld, M. M. Korshunov, and I. I. Mazin, *Rep. Prog. Phys.* **74**, 124508 (2011).
- ⁶ Fa Wang and D.-H. Lee, *Science* **332**, 200 (2011).
- ⁷ C. Löhnert, T. Stürzer, M. Tegel, R. Frankovsky, G. Friederichs, and D. Johrendt, *Angew. Chem. Int. Ed.* **50**, 9195 (2011).
- ⁸ N. Ni, J. M. Allred, B. C. Chan, and R. J. Cava, *Proc. Natl. Acad. Sci. USA* **108**, E1019 (2011).
- ⁹ S. Kakiya, K. Kudo, Y. Nishikubo, K. Oku, E. Nishibori, H. Sawa, T. Yamamoto, T. Nozaka, and M. Nohara, *J. Phys. Soc. Jpn.* **80**, 093704 (2011).
- ¹⁰ Z. J. Xiang, X. G. Luo, J. J. Ying, X. F. Wang, Y. J. Yan, A. F. Wang, P. Cheng, G. J. Ye, and X. H. Chen, *Phys. Rev. B* **85**, 224527 (2012).
- ¹¹ E. Mun, N. Ni, J. M. Allred, R. J. Cava, O. Ayala, R. D. McDonald, N. Harrison, and V. S. Zapf, *Phys. Rev. B* **85**, 100502(R) (2012).
- ¹² K. Cho, M. A. Tanatar, H. Kim, W. E. Straszheim, N. Ni, R. J. Cava, and R. Prozorov, *Phys. Rev. B* **85**, 020504(R) (2012).
- ¹³ X. P. Shen, S. D. Chen, Q. Q. Ge, Z. R. Ye, F. Chen, H. C. Xu, S. Y. Tan, X. H. Niu, Q. Fan, B. P. Xie, and D. L. Feng, *Phys. Rev. B* **88**, 115124 (2013).
- ¹⁴ S. Thirupathaiah, T. Stürzer, V. B. Zabolotnyy, D. Johrendt, B. Büchner, and S. V. Borisenko, *Phys. Rev. B* **88**, 140505(R) (2013).
- ¹⁵ H. Shakeripour, C. Petrovic, and L. Taillefer, *New J. Phys.* **11**, 055065 (2009).
- ¹⁶ N. R. Werthamer, E. Helfand, and P. C. Hohenberg, *Phys. Rev.* **147**, 295 (1966).
- ¹⁷ A. Gurevich, *Phys. Rev. B* **67**, 184515 (2003).
- ¹⁸ M. Sutherland, D. G. Hawthorn, R. W. Hill, F. Ronning, S. Wakimoto, H. Zhang, C. Proust, E. Boaknin, C. Lupien, L. Taillefer, R. Liang, D. A. Bonn, W. N. Hardy, R. Gagnon, N. E. Hussey, T. Kimura, M. Nohara, and H. Takagi, *Phys. Rev. B* **67**, 174520 (2003).
- ¹⁹ S. Y. Li, J.-B. Bonnemaïson, A. Payeur, P. Fournier, C. H. Wang, X. H. Chen, and L. Taillefer, *Phys. Rev. B* **77**, 134501 (2008).
- ²⁰ J. Lowell and J. B. Sousa, *J. Low. Temp. Phys.* **3**, 65 (1970).
- ²¹ J. O. Willis and D. M. Ginsberg, *Phys. Rev. B* **14**, 1916 (1976).
- ²² E. Boaknin, M. A. Tanatar, J. Paglione, D. Hawthorn, F. Ronning, R. W. Hill, M. Sutherland, L. Taillefer, J. Sonier, S. M. Hayden, and J. W. Brill, *Phys. Rev. Lett.* **90**, 117003 (2003).
- ²³ E. Boaknin, R. W. Hill, C. Proust, C. Lupien, L. Taillefer, and P. C. Canfield, *Phys. Rev. Lett.* **87**, 237001 (2001).

- ²⁴ C. Proust, E. Boaknin, R. W. Hill, L. Taillefer, and A. P. Mackenzie, Phys. Rev. Lett. **89**, 147003 (2002).
- ²⁵ J. K. Dong, S. Y. Zhou, T. Y. Guan, X. Qiu, C. Zhang, P. Cheng, L. Fang, H. H. Wen, and S. Y. Li, Phys. Rev. B **81**, 094520 (2010).
- ²⁶ G. E. Volovik, JETP Lett. **58**, 469 (1993).
- ²⁷ J. K. Dong, T. Y. Guan, S. Y. Zhou, X. Qiu, L. Ding, C. Zhang, U. Patel, Z. L. Xiao, and S. Y. Li, Phys. Rev. B **80**, 024518 (2009).
- ²⁸ Y. Bang, Phys. Rev. Lett. **104**, 217001 (2010).